

Nanocrystalline Tin as a Preparative Tool: Synthesis of Unprotected Nanoparticles of SnTe and SnSe and a New Route to (PhSe)<sub>4</sub>Sn

Sabine Schlecht,\* Michael Budde, and Lorenz Kienle

Max-Planck-Institut für Festkörperforschung, Heisenbergstrasse 1, 70569 Stuttgart, Germany

Received April 15, 2002

The reactions of nanocrystalline tin metal (Sn\*) with elemental selenium and tellurium and with the diaryldichalcogenides Ph<sub>2</sub>Se<sub>2</sub> and Ph<sub>2</sub>Te<sub>2</sub> have been investigated. Reaction of Sn\* with the soluble tellurium source Ph<sub>2</sub>Te<sub>2</sub> led to a clean formation of nanoparticles of cubic SnTe. Dependent on the concentration of Ph<sub>2</sub>Te<sub>2</sub>, the particles sizes could be varied between 15 and 60 nm in average, whereas the reaction of Sn\* with Ph<sub>2</sub>Se<sub>2</sub> formed molecular Sn(SePh)<sub>4</sub> in high yield. The latter molecular compound was thermolyzed at 300 °C, yielding nanocrystalline SnSe with a broader distribution of size. The nanoparticles of SnTe were thoroughly investigated by transmission electron microscopy (TEM) and powder X-ray diffraction. The reactions of Sn\* with elemental selenium and tellurium gave single-phase but microcrystalline SnSe and SnTe.

## Introduction

The IV/VI semiconductor compounds such as PbSe, SnSe, and SnTe are widely applied in IR detectors<sup>1</sup> and as thermoelectric materials,<sup>2</sup> and SnS is discussed as a possible photoactive layer in solar cells.<sup>3–5</sup> In contrast to the multitude of syntheses for nanoparticles of II/VI semiconductors<sup>6,7</sup> there is only a small variety of synthetic routes to IV/VI semiconductor nanoparticles. Some of them involve the use of an autoclave and liquid ammonia or other amines as solvents to activate the chalcogen.<sup>8–10</sup> We have developed a new approach to tin chalcogenide nanoparticles starting from nanocrystalline-activated tin metal. So far, similar elemental-direct reactions<sup>11</sup> leading to nanoparticles have only been reported for II/VI semiconductors.<sup>11,12</sup>

\* To whom correspondence should be addressed. E-mail: schlecht@jansen.mpi-stuttgart.mpg.de.

- (1) Unger, K. *Verbindungshalbleiter*; Akademische Verlagsanstalt: Leipzig, Germany, 1986.
- (2) Dresselhaus, M. S.; Dresselhaus, G.; Sun, X.; Zhang, Z.; Cronin, S. B.; Koga, T.; Ying, J. Y.; Chen, G. *Microscale Therm. Eng.* **1999**, *3*, 89.
- (3) Nair, M. T. S.; Nair, P. K. *Semicond. Sci. Technol.* **1991**, *6*, 132.
- (4) Prince, M. B. *J. Appl. Phys.* **1955**, *26*, 534.
- (5) Loferski, J. J. *J. Appl. Phys.* **1956**, *27*, 777.
- (6) Trindade, T.; O'Brien, P.; Pickett, N. L. *Chem. Mater.* **2001**, *13*, 3843.
- (7) Malik, M. A.; O'Brien, P.; Revaprasadu, N. *S. Afr. J. Sci.* **2000**, *96*, 55.
- (8) Henshaw, G.; Parkin, I. P.; Shaw, G. *J. Chem. Soc., Dalton Trans.* **1997**, 231.
- (9) Li, Y.; Wang, Z.; Ding, Y. *Inorg. Chem.* **1999**, *38*, 4737.
- (10) Wang, W.; Geng, Y.; Yan, P.; Liu, F.; Xie, Y. *J. Am. Chem. Soc.* **1999**, *121*, 4062.
- (11) Li, Y.; Liao, H.; Ding, Y.; Fan, Y.; Zhang, Y.; Qian, Y. *Inorg. Chem.* **1999**, *38*, 1382.

## Experimental Section

All manipulations were carried out under dry, oxygen-free argon, except where stated otherwise. Li[Et<sub>3</sub>BH], 1 M in tetrahydrofuran (THF), diethylene glycol dimethyl ether (anhydrous), diphenyl diselenide, and diphenyl ditelluride were purchased from Aldrich, and SnCl<sub>2</sub> (anhydrous), selenium, and tellurium were obtained from Merck. All chemicals were used without further purification. THF was purchased from Merck and distilled over CaH<sub>2</sub> under an argon atmosphere.

Powder X-ray diffraction data were collected using a STOE-Stadi P diffractometer (germanium monochromator, Cu K $\alpha$  radiation,  $\lambda$  = 1.540 56 Å, linear position sensitive detector, silicon as an external standard).

The sample was characterized by high-resolution electron microscopy (HREM) and selected area electron diffraction (SAED). The particles were dispersed in *n*-butanol. One drop of the suspension was placed on a perforated carbon/copper net, which was dried carefully, leaving the particles in random orientations. The electron microscopy studies were performed with a Philips CM30/ST instrument equipped with a LaB<sub>6</sub> cathode. At 300 kV, the point resolution is 0.19 nm. SAED patterns were obtained using a diaphragm that limited the diffraction to a circular area of 125 nm in diameter. Kinematical SAED patterns were calculated with the EMS program package. Working with the Philips CM30/ST, X-ray analyses (mapping and EDX point measurements) were carried out using a Noran SiLi detector and the Vantage DSI system (Noran). EDX analyses were also performed applying the SE mode

- (12) Li, Y.; Ding, Y.; Qian, Y.; Zhang, Y.; Yang, L. *Inorg. Chem.* **1998**, *37*, 2844.

of a Philips XL30 ESEM scanning electron microscope (acceleration voltage, 25 kV). For the latter analyses, a small amount of the tin chalcogenide was placed on an adhesive graphite foil.

**Elemental Direct Reaction of Nanocrystalline Tin with Selenium or Tellurium.** A 190 mg sample of  $\text{SnCl}_2$  was dissolved in 60 mL of THF and reduced at room temperature by 2.0 mL of a 1.0 M solution of  $\text{Li}[\text{Et}_3\text{BH}]$  in THF.<sup>13</sup> The reaction mixture was stirred for 15 min, and then the THF was decanted and substituted by 60 mL of diglyme. Then 77 mg (1.0 mmol) of elemental selenium was added and the suspension was heated to 125 °C for 24 h. It was allowed to cool to room temperature, and the precipitate was filtered off and washed twice with 10 mL of THF. The  $\text{SnSe}$  was dried under vacuum and stored at room temperature in air.

The reaction of  $\text{Sn}^*$  with tellurium was performed by following the same protocol but with a reaction temperature of 85 °C.

**Synthesis of  $\text{SnTe}$  Nanoparticles.** Nanocrystalline tin metal was obtained according to ref 13. A 190 mg (1.0 mmol) amount of  $\text{SnCl}_2$  was dissolved in anhydrous THF, and 2.0 mL of a 1.0 M solution of  $\text{Li}[\text{Et}_3\text{BH}]$  was added. Immediate precipitation of nanocrystalline tin was observed. The reaction mixture was stirred for 15 min and then allowed to settle. The supernatant was decanted, and the tin was washed with THF and dried under vacuum. The black powder (1.0 mmol) was suspended in 60 mL of anhydrous diglyme. A 409 mg (1.0 mmol) amount of diphenyl ditelluride were added and dissolved immediately. The suspension was heated to 165 °C (gentle boiling of the diglyme solvent) for 2 h. The color of the solution gradually changed from light orange to orange-red. The reaction mixture was allowed to cool, and the precipitate was filtered off and washed with  $3 \times 5.0$  mL of THF. The  $\text{SnTe}$  nanoparticles were dried under vacuum and stored in air at room temperature.

The same sequence of reactions was conducted starting from 19 mg (0.1 mmol) of  $\text{SnCl}_2$  in 100 mL of anhydrous THF and subsequent conversion of as-prepared tin with 41 mg (0.1 mmol) of  $\text{Ph}_2\text{Te}_2$  in 60 mL of diglyme at 165 °C for 2 h. Thus obtained smaller  $\text{SnTe}$  nanoparticles were centrifuged from the solution, washed, and dried under vacuum.

Amorphous  $\text{SnSe}$  was obtained from activated tin metal (1.0 mmol) and  $\text{Ph}_2\text{Se}_2$  (1.0 mmol) by following the same protocol.

**Synthesis of  $\text{Sn}(\text{SePh})_4$ .** A 119 mg sample (1.0 mmol) of activated tin was suspended in 50 mL of THF. A 624 mg (2.0 mmol) amount of diphenyl diselenide was added, and the reaction mixture was heated under reflux for 15 h. It was allowed to cool to room temperature, a very small amount of residual tin was filtered off, and the solvent was evaporated to dryness under vacuum.  $\text{Sn}(\text{SePh})_4$  was obtained as a yellow powder in 94% yield. Elemental analysis, powder diffraction data, and NMR spectroscopic data were in full accordance with the literature<sup>14</sup> and with the composition  $\text{C}_{24}\text{H}_{20}\text{Se}_4\text{Sn}$ .

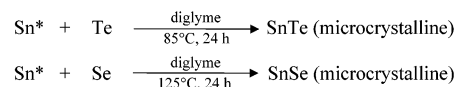
**Pyrolysis of  $\text{Sn}(\text{SePh})_4$ .** A 372 mg (0.5 mmol) amount of  $\text{Sn}(\text{SePh})_4$  was placed at the bottom of a long Schlenk tube equipped with a bubbler for pressure release. The bottom half of the Schlenk tube was immersed in an electrical oven and heated to 300 °C. This temperature was held for 30 min. The formation of a black solid from the  $\text{Sn}(\text{SePh})_4$  melt and the condensation of the volatiles in the top part of the Schlenk tube started around 130 °C. The Schlenk tube was allowed to cool to room temperature, and the black powder ( $\text{SnSe}$ ) at the bottom was taken out mechanically. It

was stored in air at room temperature. Powder diffraction data were in accordance with JCPDS 48-1224 for  $\text{SnSe}$ .

## Results and Discussion

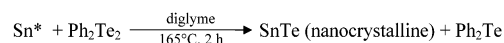
Solvochemically activated tin ( $\text{Sn}^*$ ) was obtained from  $\text{SnCl}_2$  and  $\text{Li}[\text{Et}_3\text{BH}]$  as a reducing agent.<sup>13</sup> As-prepared activated tin was reacted at low temperatures with elemental selenium and tellurium (Scheme 1).

**Scheme 1**



Single-phase  $\text{SnSe}$  ( $Pbnm$ ) and  $\text{SnTe}$  ( $Fm\bar{3}m$ ) were obtained in quantitative yield after 24 h. These products represent the thermodynamically stable modifications of the respective compounds.<sup>15</sup> The given reaction temperatures of 85 °C for tellurium and 125 °C in the case of selenium represent the lowest possible temperatures at which a complete conversion into the tin chalcogenide occurred. In contrast to the analogous synthesis of  $\text{SnS}$ ,<sup>16</sup> the products are not nanocrystalline but microcrystalline. Our experience with the synthesis of  $\text{SnS}$  nanoparticles suggested that the chalcogen that is used in the reaction needs to be soluble in diglyme (diethylene glycol dimethyl ether) solvent to give a nanocrystalline product. Therefore, we used diphenyl ditelluride,  $\text{Ph}_2\text{Te}_2$ , and diphenyl diselenide,  $\text{Ph}_2\text{Se}_2$ , as soluble chalcogen sources. Reaction of  $\text{Ph}_2\text{Te}_2$  with nanocrystalline tin metal at 165 °C gave single-phase nanocrystalline  $\text{SnTe}$  and diphenyl telluride,  $\text{Ph}_2\text{Te}$  (Scheme 2). When the same

**Scheme 2**



reaction was conducted in boiling THF (68 °C), a conversion to  $\text{SnTe}$  still took place but the product was amorphous.

The nanoparticles can be separated from the solution of the liquid byproduct by simple filtration. The nanosized  $\text{SnTe}$  particles were characterized by X-ray powder diffraction (XRD), EDX analysis, and transmission electron microscopy (TEM).

When nanocrystalline  $\text{SnTe}$  is synthesized from nanocrystalline tin and a soluble source of tellurium, the question arises how the particle size and shape of the product depend on the size of the tin particles and the concentration of the tellurium source. We tried to vary the particle size of the nanocrystalline tin by a change of the concentration of  $\text{SnCl}_2$  in THF before the reduction with  $\text{Li}[\text{Et}_3\text{BH}]$ . Strikingly, no effect on the particle size was observed when the concentration of the solution of  $\text{SnCl}_2$  was reduced from 10 to 1 mM. In both cases, tin particles of 40–50 nm size were obtained (see Supporting Information).

For the conversion of  $\text{Sn}^*$  to nanocrystalline  $\text{SnTe}$  two different reaction conditions, named A and B in the following, were applied (Scheme 3).

(13) Bönemann, H.; Brijoux, W.; Joussen, T. *Angew. Chem., Int. Ed. Engl.* **1990**, *29*, 273.

(14) Barton, D. H. R.; Dadoun, H. *New J. Chem.* **1982**, *6*, 53.

(15) Wiedemeier, H.; von Schnering, H.-G. *Z. Kristallogr.* **1978**, *148*, 295.

(16) Schlecht, S.; Kienle, L. *Inorg. Chem.* **2001**, *40*, 5719.

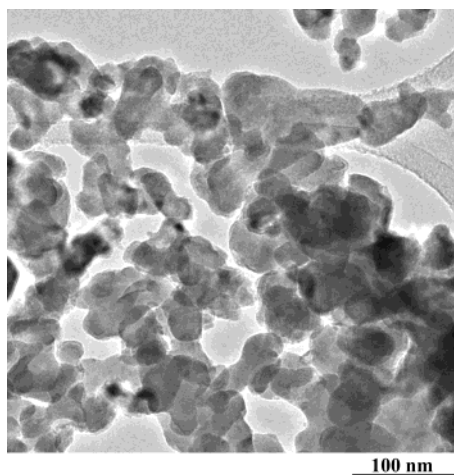


**Figure 1.** Typical micrograph of round SnTe nanocrystals (60 nm average size).

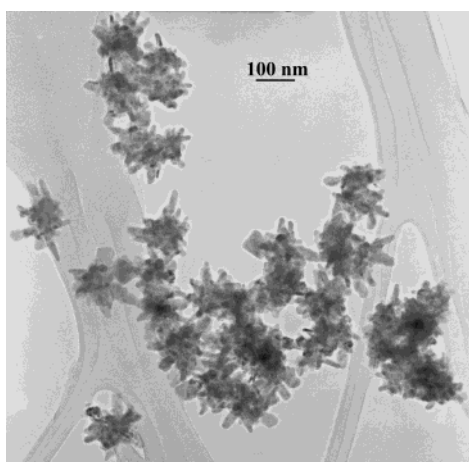
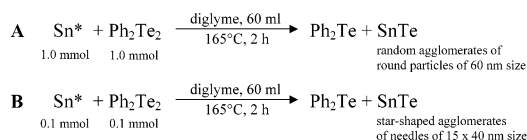


**Figure 2.** Typical micrograph of star-shaped agglomerates of SnTe needles ( $15 \times 40$  nm average size).

### Scheme 3



Under conditions A, when 1.0 mmol of nanocrystalline tin and 1.0 mmol of  $\text{Ph}_2\text{Te}_2$  in 60 mL of diglyme were used, large agglomerates of randomly oriented particles of about 60 nm size were obtained (Figure 1). Under conditions B, with only 0.1 mmol of  $\text{Sn}^*$  and  $\text{Ph}_2\text{Te}_2$  in the same amount of solvent, the reaction yielded smaller star-shaped agglomerates of needles with an average size of  $15 \times 40$  nm (Figure 2).

The powder diffraction diagram for tin telluride nanoparticles prepared by route A and the reflections for bulk cubic SnTe (JCPDS 46-1210) are shown in Figure 3. All reflections in the powder diffraction diagram for the nanoparticles were indexed, and the obtained lattice parameter of  $a = 6.329(2)$  Å is identical within the standard deviation with the published value of  $a = 6.3275(5)$  Å for bulk SnTe. No other crystalline phase was observed. EDX analysis of the nanoparticles confirmed a 1:1 ratio of tin and tellurium. A mean crystallite

size of 60 nm was derived from the reflections using Scherrer's equation.<sup>17</sup>

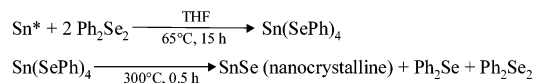
The TEM micrograph in Figure 1 gives an overview of the round SnTe nanoparticles. It confirms the average particle size obtained from powder diffraction data. No amorphous byproducts can be found according to electron diffraction and TEM micrographs. The EDX analyses confirm the expected composition (SnTe); no inhomogeneities were observed in the nanocrystals using X-ray mapping.

Most of the particles are highly crystalline and do not exhibit any crystal defects. Hence, the electron diffraction patterns are characterized by Bragg reflections only. A high-resolution electron micrograph of a SnTe nanoparticle and the corresponding SAED pattern (zone axis  $[110]$ ) are depicted in Figure 4. Patterns taken from thin regions of the nanocrystals agree convincingly with simulated kinematical patterns (see Figure 4a,b). In rare cases twin boundaries were observed in the nanocrystals. A typical example is shown in Figure 5 for zone axis  $[110]$ . All indices refer to the zone axis orientations of the single domains. The positions of the Bragg intensities in the SAED pattern of the twinned crystal can be constructed by superimposing two patterns with  $[110]$  zone axis (see Figure 5b for the experimental pattern and Figure 5a for the construction). The *mmm*-symmetry of the superimposed pattern offers two possibilities for the twin law: a reflection perpendicular to the directions  $[122]^*$  or  $[11\bar{1}]^*$  of the reciprocal space (see Figure 5a,b). For the unambiguous determination of the twin law the direct space can be analyzed using HREM. Figure 5c indicates the orientations of both twin domains (see arrows marking  $[001]$ ) which are connected by a reflection perpendicular to  $[11\bar{1}]$ . Between the two domains a narrow region of overlapping domains is observed.

The smaller, more needlelike particles prepared by route B were also investigated by TEM and compared to the ones obtained via route A. Figure 6 shows a high-resolution electron micrograph of one of the needles and the corresponding SAED pattern (zone axis  $[110]$ ). Like the round particles, the needles are also highly crystalline and exhibit very few defects.

In contrast to the tellurium system, the analogous reaction of  $\text{Sn}^*$  with  $\text{Ph}_2\text{Se}_2$  at  $165^\circ\text{C}$  for 2 h led to amorphous tin selenide SnSe in quantitative yield. To obtain nanocrystalline SnSe the reaction had to be conducted in two separate steps (Scheme 4).

### Scheme 4



In the first step, nanocrystalline tin metal was reacted with 2 equiv of diphenyl diselenide,  $\text{Ph}_2\text{Se}_2$ , at only  $65^\circ\text{C}$  in THF, and under these conditions the tin was cleanly converted into the molecular addition product  $\text{Sn}(\text{SePh})_4$ . As in the alternative synthesis of  $\text{Sn}(\text{SePh})_4$ ,<sup>15</sup> the product is formed as a

(17) Guinier, A. *X-ray Diffraction in Crystals, Imperfect Crystals, and Amorphous Bodies*; Dover: New York, 1994; Chapter 5, p 121.

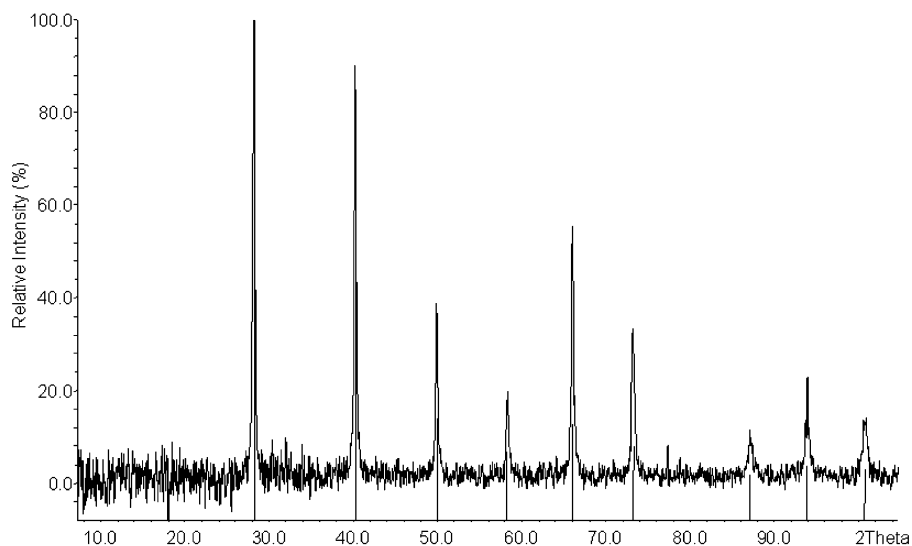


**Figure 3.** Powder diffraction pattern for 60 nm SnTe nanoparticles with reflections indexed for cubic SnTe (JCPDS 46-1210).

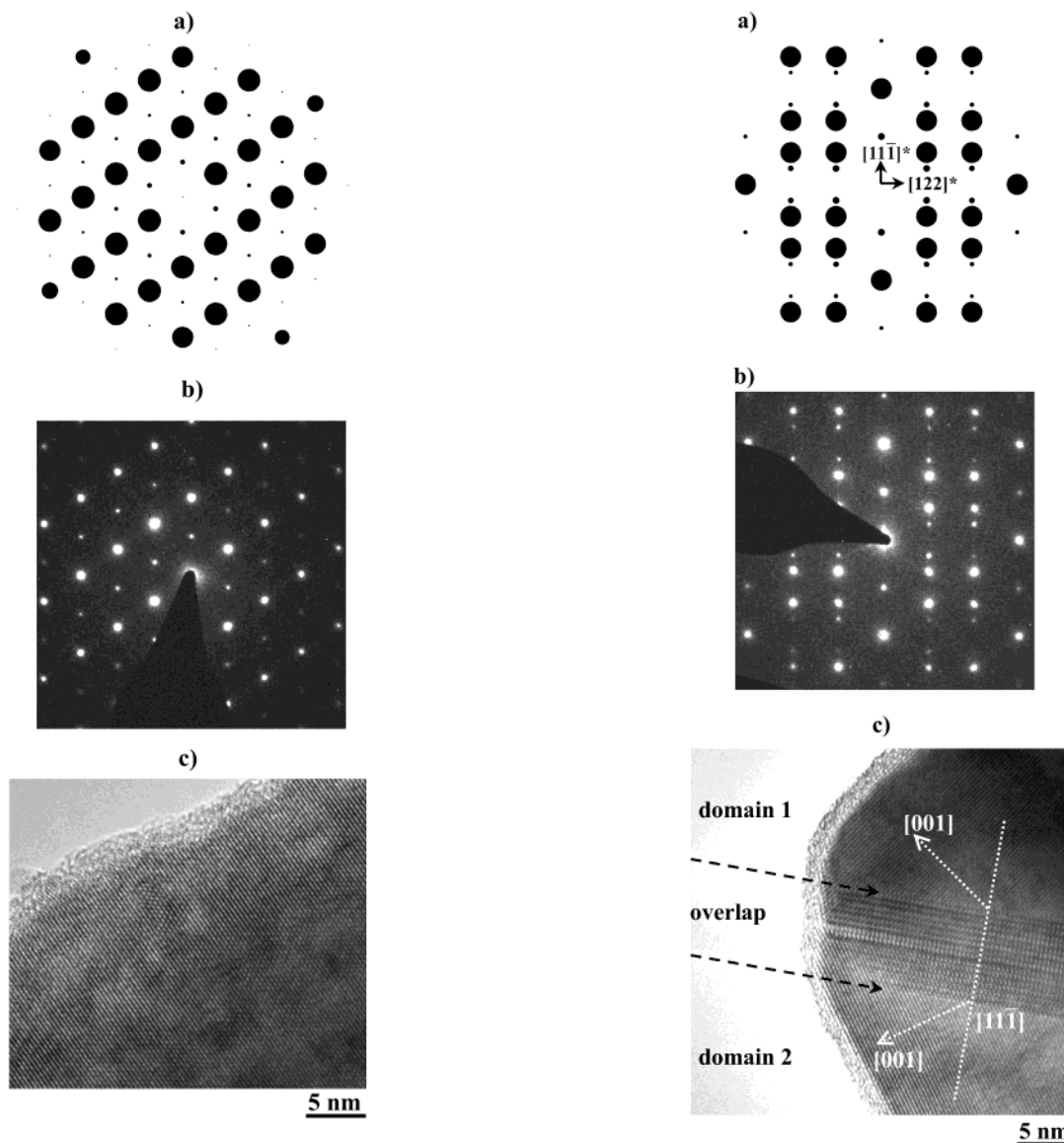


**Figure 4.** HREM micrograph and SAED pattern for a round 60 nm SnTe nanoparticle, zone axis  $[110]$ : (a) simulated pattern; (b) experimental pattern; (c) HREM micrograph.

**Figure 5.** Twinning of SnTe nanocrystals: (a) construction of the superimposed patterns; (b) experimental pattern; (c) HREM micrograph indicating the orientation of the twin boundary, where black arrows mark the region with overlapping domains 1 and 2.



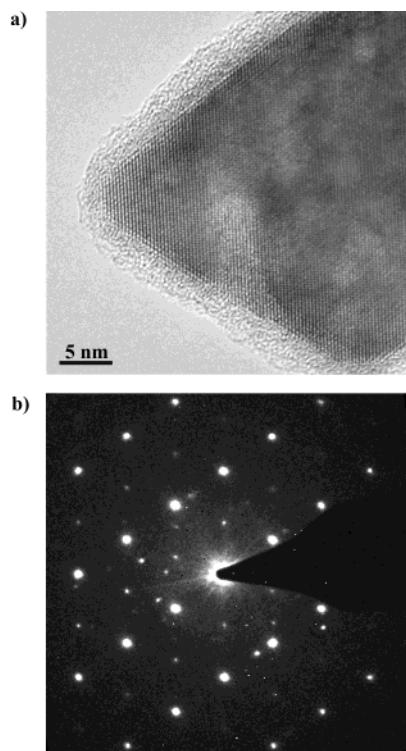


**Figure 6.** HREM micrograph and SAED pattern for a SnTe needle, zone axis [110]: (a) HREM micrograph; (b) SAED experimental pattern.

mixture of both its known polymorphs but with much higher yield (94% compared to 60%). In a second step, a short pyrolysis of  $\text{Sn}(\text{SePh})_4$  at 300 °C led to nanocrystalline SnSe and to the elimination of the organoselenium compounds  $\text{Ph}_2\text{Se}_2$  and  $\text{Ph}_2\text{Se}$ .

In contrast to the SnTe nanoparticles produced from activated tin and  $\text{Ph}_2\text{Te}_2$ , these SnSe nanoparticles show a broad dispersion with particle sizes from 3 up to 50 nm.

Prolonged pyrolysis of the molecular precursor  $\text{Sn}(\text{SePh})_4$  at 300 °C led to big annealed particles that were no longer nanocrystalline. For all types of SnSe products (amorphous, nanocrystalline, and microcrystalline SnSe) EDX analysis confirmed a Sn:Se ratio of 1:1.

None of the reactions reported herein could be performed with commercial microcrystalline tin powder under the given reaction conditions.

### Summary

We have shown that activated nanocrystalline tin can be used as a preparative tool for the synthesis of tin chalcogenide nanoparticles nc-SnX with X = S,<sup>16</sup> Se, and Te. The whole family of chalcogenides could be prepared by this general synthetic approach, starting from an activated group 14 element instead of an activated chalcogen. In the case of the SnTe nanoparticles it could be shown that particle size and shape depend on the concentration of the reactants and can therefore be controlled by an appropriate choice of these concentrations. More detailed investigations of this concentration dependence and of the nucleation and growth of the SnTe particles in this type of reaction are currently under way.

**Acknowledgment.** We are especially grateful to Viola Duppel for her help with the TEM micrographs and to Prof. Dr. Arndt Simon for providing the transmission electron microscope. S.S. thanks the Fonds der Chemischen Industrie and the BMBF for a Liebig-Fellowship and Prof. Dr. Martin Jansen for his continuous support.

**Supporting Information Available:** Several TEM micrographs and SAED patterns of the tin nanoparticles that were used as starting materials. This material is available free of charge via the Internet at <http://pubs.acs.org>.

IC020272Y